

Diagnostic Potentials of FT-IR Microspectrometry in the Examination of Colorectal Adenocarcinomas

Peter Lasch

Robert Koch-Institut, P25 Biomedical Spectroscopy, 13353 Berlin, Nordufer 20, Germany

1. Introduction

The past decade has witnessed substantial progress towards the application of infrared microspectrometry as an useful diagnostic tool for spectroscopic characterization of histological specimens. The combination of IR spectroscopy with microscopy, new technical developments such as sensitive multichannel detectors, and the implementation of modern multivariate concepts of data analysis permit high-quality infrared microspectroscopic imaging of tissue samples. The IR imaging methodology provides spatially resolved structural and compositional information of the histological specimens and opens in combination with computer based multivariate image reassembling techniques wide perspectives for routine use in the clinical environment.

After 15 years of research it is now an accepted standard that IR spectra of cells, or tissues, can be considered as complex spectral fingerprints which cannot be always completely understood in an analytical sense. It is therefore advantageous to analyze the spectral fingerprints by pattern recognition techniques, preferentially of the supervised type, such as multilayer perceptron artificial neural networks (MLP-ANN), or support vector machines (SVM). As the concept of supervised classification requires a training, or teaching phase, in which labeled subsets of tissue reference spectra are analyzed, the compilation and validation of the teaching spectra will be the main challenge to render IR microspectroscopic expert systems applicable in practice. Thus, it is believed that the development of a non-subjective IR based tissue characterization technique will be dependent on the collection of databases of teaching spectra ideally containing a representative number of standardized spatially resolved IR microspectra of all relevant normal and pathologic tissue structures.

The aforementioned aspect is important because despite all the fascinating perspectives, promising technical developments and exciting research papers, progress towards the translation of the technique into a practical application is less evident. The lack of available spectral reference databases is now identified as a factor which limits the transfer of the technique from the research laboratory to the clinical environment. In our presentation we will consequently discuss a number of topics relevant to the collection of spectral databases: the definition of measurement standards, measurement conditions and of quality control criteria for IR microspectrometry of tissues. The main focus of this presentation, however, is on the presentation of basic principles of data evaluation in IR microspectroscopic imaging of tissues.

2. Concepts of data analysis in mid-IR microspectrometric imaging of tissues

Fourier Transform Infrared (FT-IR) microspectrometry provides spatially resolved structural and compositional information of the histological specimens under investigation and shows in

combination with digital imaging techniques a great promise for in-vivo and ex-vivo medical diagnosis. False color images produced by IR image segmentation methodologies are directly comparable to outcomes of standard histological staining protocols and can be interpreted also by non-spectroscopists. A number of different IR imaging strategies have been proposed in the past. Among them, the univariate concept of chemical imaging still enjoys great popularity. Chemical imaging is based on the reduction of an array of infrared spectra (known as the spectral hypercube) to a functional group map [1]. Chemical images are easy to generate and, from a spectroscopic point of view, also easy to interpret. The main drawback of the technique is that only a small fraction of the available spectral information is employed [2,3]. Nevertheless, it is well-documented for a number of examples that functional group mapping produces sufficiently high image contrast and permits visualization of the spatial distribution of defined tissue structures [4-6].

We found, however, that one spectral feature is oftentimes inadequate as a sole differentiation criterion, particularly if spectral data of several patients are analyzed [7-9]. Several techniques of multivariate imaging attempt to address this shortcoming by analyzing large fractions or even the complete spectral information. Among multivariate imaging methods, unsupervised techniques became popular because they allow to produce IR images with the full spectral contrast that often corresponds to the classical histopathological scheme. Specifically, various types of cluster analysis and among them agglomerative hierarchical clustering (AHC) in a combination of a correlation distance measure (D-values) and Ward's clustering method turned out to be particularly suitable for IR image segmentation. In a comparative study of cluster imaging techniques it was shown for example, that the highest degree of correspondence between histopathology and IR spectroscopy was achieved when the AHC algorithm was applied [10]. The major drawback of the AHC segmentation technique are the very high computing requirements, which become more and more relevant when large spectral data sets have to be analyzed. Compared with the AHC technique, k-means and fuzzy-C-means clustering turned out to be less efficient image segmentation methods but have the advantage of lower computational efforts [10].

An important characteristic of unsupervised clustering methods is the tendency to partition the data according to the overall spectral variance. In view of the fact that usually only a small fraction of a sample's spectral variance will be *intra-class* specific, the clustering strategy is particularly efficient if spectra of only one patient are analyzed. On the other hand, if more than one sample is examined, the *intra-class* variance includes also the variance of various patients. In these cases, the *intra-class* variance may be at the order of the *inter-class* variance which is the main reason why unsupervised classification methodologies are not ideally suited to analyze spectral databases. In this paper, we will however demonstrate, that unsupervised classification techniques are invaluable explorative tools for the development of supervised classification models.

It has been noticed earlier that supervised classification strategies e.g. by multilayer-perceptron (MLP) artificial neural network models with supervised learning are the techniques of choice for the development of effective and robust classifiers for IR based classification of tissues [8]. It is a strength of this approach that supervised techniques can be efficiently optimized by pre-selecting appropriate spectral features from the complete spectral data [11,12]. Furthermore, the classification accuracy of the above-mentioned combination of methods will strongly depend on the type of spectral preprocessing. We found that spectral quality tests, baseline correction

(derivatives) and normalization of the raw spectral data are essential prerequisites for the development of robust classification models [7,8,].

The outlined classification strategy of a preceding spectral preprocessing followed by feature selection and artificial neural network classification is based on a extraordinary high number of free variables, i.e. over-fitting of the prediction models is a real risk [11,12]. Thus, it is absolutely necessary to evaluate the model by independent sets of spectral patterns which must not be used when designing the model [11,12]. Consequently, the model development should be based on the well-known concept of independent (external) validation: it is required to split the database into spectral subsets for teaching, a subset for internal validation and a completely independent - ideally blinded - subset for external validation (testing). Thus, the process of model development - and this includes also the selection of the spectral features - should be carried out exclusively on the basis of the teaching and internal validation data subsets. It should be emphasized that this strategy is the only way to reveal over-fitting of the model and to obtain objective values of diagnostic test parameters (sensitivity, specificity, etc.) [11,14].

In the following we will present results obtained from the analysis of about 1.5 million FT-IR microspectra from human colorectal adenocarcinoma specimens. Based on these data we exemplarily demonstrate how a database of colorectal reference spectra can be established and which strategy of spectral analysis should be used for precise and efficient classification of IR microspectroscopic imaging data.

3. The colon database of point spectra

Colorectal adenocarcinoma tissue samples from 28 patients were obtained from the tissue data bank at the Robert-Rössle-Clinic at the Max-Delbrück-Centrum for Molecular Medicine in Berlin. They originated from coecum, colon ascendens, transversum or descendens, sigma and rectum and the histopathological grade of malignancy was established as well differentiated (G1), moderately differentiated (G2), or poorly differentiated (G3).

Infrared microspectra were acquired from cryo-sectioned specimens. Altogether, spectra from 35 infrared spectral maps and 28 patient samples have been collected (see Ref. [15] and chapters 8.1. and 8.2. for details of sample preparation and IR data collection). In order to extract point spectra from the IR tissue maps we have routinely applied the approach of agglomerative hierarchical cluster (AHC) imaging to all individual spectral maps (see chapter 8.5 for details). AHC images and the histoarchitecture of the post-stained tissue sections allowed subsequent identification of specific histopathological structures within the maps. We have used this information to extract a representative number of point spectra, usually between 10 - 15 per map and cluster. The extracted point spectra were then used to build up a database of IR colon reference microspectra from the histologically defined structures of interest. The colon database contained spectra from many patients, so that *inter-class* as well as the *intra-class* variance were adequately represented. An overview of the database is given in Table 1.

	class name	# of database spectra
Ia	crypts	153
Ib	mucin	385
IIa	necrosis	169
IIb	lamina propria mucosae	128

IIc	lymphocytes	41
IIIa	tunica muscularis	138
IIIb	lamina muscularis mucosae	170
IIIc	vessel (blood, lymph)	193
IVa	submucosa	34
IVb	fibrovascular connective tissue	878
V	adenocarcinoma	1805
VI	fat tissue	26

Table 1. The colon database. Class definitions and number of spectra per class.

4. The importance of standardization

Standardization of the measurement conditions and measurement parameters are considered as a necessary precondition for the transfer of the IR imaging technology into a practical application. It should be self-evident that IR spectral databases require consistent IR spectral profiles of measured tissue structures. In the following we will therefore discuss a number of factors with potential impact on the spectral reproducibility, among them methods of sample preparation, of the optical setup, type of optical substrates, and the spectral and spatial resolution.

Sample preparation: In the last 15 years a number of techniques for mid-IR compatible preparation of tissue samples have been suggested, among them sectioning of paraffin-embedded tissue blocks and cryo-sectioning of snap frozen tissue samples for transmission, or transflection type IR microspectrometry. We at the Robert-Koch-Institute favor for reasons of simplicity, practicality and reproducibility cryo-sectioning at temperatures between -18 and -22°C. Usually, tissue sections of a thickness of 8 µm are produced by a cryostat. This avoids the need of deparaffinization with xylol or alcohol which is known to partly remove several classes of lipids and to induce conformational changes of proteins. Furthermore, a thickness of 8 µm is advantageous because it allows to produce relatively large tissue sections. For the preferred transmission type measurements we found also that a thickness of 8 µm gives ideal absorbance values of approx. 0.8 in the amide I region. This avoids misinterpretations of spectral artifacts in the amide I region (non-linearity of MCT detector response if the sample is too thick) and assures at the same time a high spectral signal-to-noise-ratio (SNR).

Optical material: After cryo-sectioning the tissue slices are routinely mounted on CaF₂ windows of a thickness of 1 mm. The window material is used because it is nearly insoluble in water and thus allows post-staining of the sections by Hematoxylin and Eosin (H&E). Compared with other window materials such ZnSe or KRS-5 the refractive index of CaF₂ is relatively low, so that the extend of optical fringing and chromatic aberrations introduced by the window material are reduced (see Ref. [16] for details). Finally, CaF₂ is colorless in the visible spectral range which allows effective documentation of the post-stained specimens (note the properties of Si, Ge, ZnSe and KRS-5 in the vis region). These properties qualify CaF₂ as a material with excellent spectral properties for biomedical spectroscopy. Disadvantages of CaF₂ are the low-frequency cutoff at ca. 950 cm⁻¹ (1 mm thickness) and costs of approximately 150 € per window. Less expensive supporting substrates such as thin PEN (polyethylene naphthalate, Du Pont) or PET films (polyethylene terephthalate, Du Pont) have been also tested in our laboratory. Unfortunately, these materials exhibited in the spectral region of interest sharp absorption bands of high intensity which could not be fully compensated by spectral subtraction.

Water vapor, carbon dioxide: All infrared instruments in our laboratories, including the IR microscopes, are equipped with home-made plexiglass boxes that can be purged with dry air. This, and a stable concentration of carbon dioxide are considered as essential prerequisites for reproducible spectra acquisition. In this context it is of particular importance that the long optical pathlengths in IR microspectrometers and the high extinction coefficients of water vapor can result in very low transmission of IR light at the water vapor absorption lines between 1400 - 1800 cm^{-1} . These effects are oftentimes overlooked due to the intrinsic low half-widths of water vapor bands and the low spectral resolution of 4, or 8 cm^{-1} , commonly used in biomedical IR spectroscopy. Nevertheless, sharp water vapor lines have a strong impact on the spectral quality (SNR) in the region of 1400 - 1800 cm^{-1} and cannot be compensated by software algorithms alone. Thus, it has been our strategy to reduce spectral contributions from water vapor by effective purging of all IR instruments.

Spectral resolution: In order to test for the ideal spectral resolution in FT-IR microspectrometry of tissue sections a series of test measurements with varying settings for spectral resolution (RES) and a computational parameter, the zero-filling factor (ZFF), was carried out. The results of these tests carried out ten years ago are shown in Figure 1.

The derivative spectra of Figure 1 demonstrate, that most of the "real" spectral features of an arbitrary tissue area are discernible at a spectral resolution of $\text{RES} = 6 \text{ cm}^{-1}$ and a $\text{ZFF} = 4$. Since the spectral resolution defines the maximum retardation of a spectrum measured interferometrically, the total time of a scan depends on the resolution: the lower the resolution the lower the time required to collect a spectrum. The second factor ZFF is a entirely computational parameter and defines the number of zero values which are added to the side lobes of an interferogram before Fourier transformation. Note that zero filling corresponds to an interpolation and does not add any structural information. We found, however, the ZFF important for subsequent Savitzky-Golay derivation which is routinely applied in spectral preprocessing. In conclusion we found at values of $\text{RES} = 6$ and $\text{ZFF} = 4$ most of the spectral details adequately resolved. This combination allowed rapid collection of FT-IR spectra at a reasonable SNR. It should be emphasized however, that other factors such as the apodization function, or the type of interferometer may also influence the effective spectral resolution.

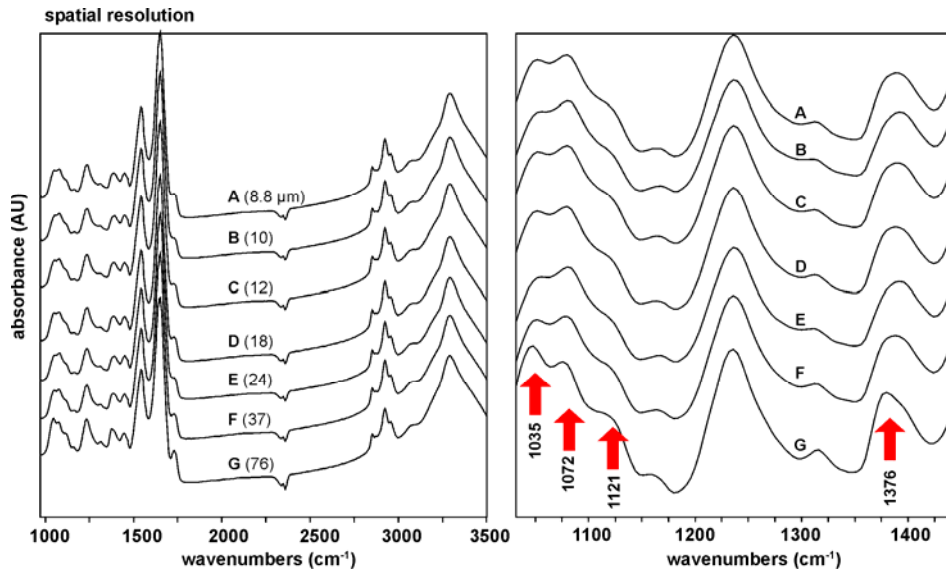


Figure 1. The influence of the parameter of spectral resolution (RES) and the zero filling factor (ZFF) on the detectability of IR spectral features of tissues. In this example, identical positions of a tissues sample mounted on a CaF_2 window of a thickness of 1 mm were characterized utilizing a Bruker IR Scope II infrared microscope. Transmission type IR spectra were recorded using a circular aperture of $100\ \mu\text{m}$ diameter. A Happ-Genzel apodization function and a variable number of scans (e.g. 512 for $\text{RES} = 1\ \text{cm}^{-1}$) was applied. Absorbance spectra were transformed by Savitzky-Golay derivation with 9 smoothing points (adapted from Ref. [17]).

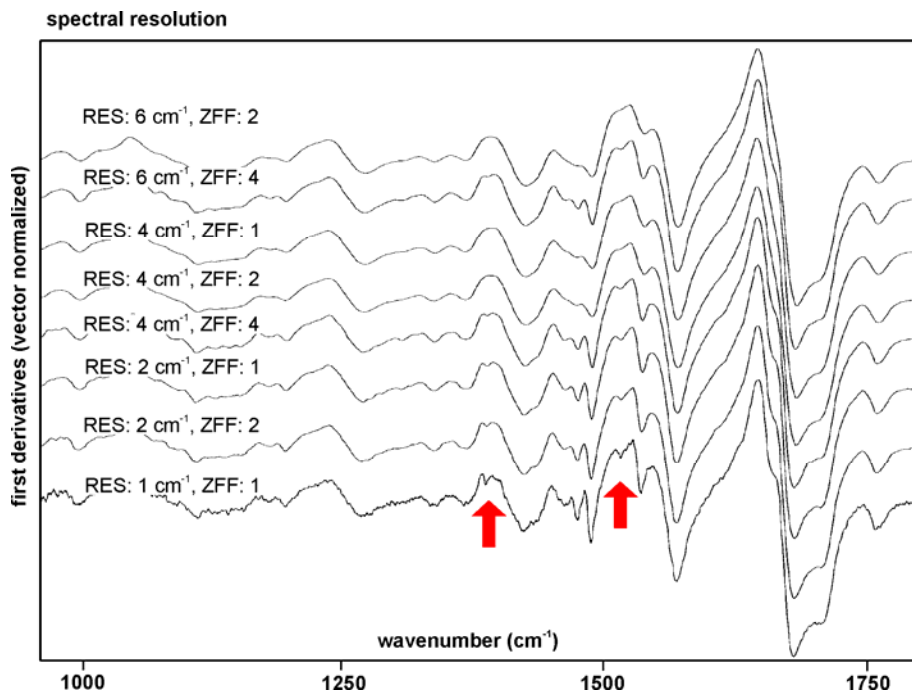


Figure 2. Computational example of a variation of the parameter of spatial resolution (SR) on mid-IR spectral patterns of tissues. The SR of an original map of IR point spectra ($\text{SR}: 8.8\ \mu\text{m}$ at $4000\ \text{cm}^{-1}$) was computationally reduced by pixel binning. The illustration shows class average spectra of the class "colonocytes" as a variable of the SR (traces A: $8.8\ \mu\text{m}$ - G: $76\ \mu\text{m}$). Note the spectral "contamination" of the colonocyte spectra by absorption bands of carbohydrates (mucin, see red arrows [18]).

Spatial resolution (SR): In biomedical IR microspectrometry the spatial resolution is one of the most critical measurement parameters. Due to the distinct levels of morphologic heterogeneity in cells and tissues the spatial resolution in a given IR imaging setup strongly affects the character of the infrared spectral patterns obtained from the biomedical samples. This is of particular importance when spectral data bases of reference microspectra from defined tissue structures are collected.

Figure 2 exemplary illustrates how the SR may affect the patterns of tissues microspectra. The illustration shows spectral changes of mean cluster spectra of the cluster "colonocytes" as a function of spatial resolution. In this example, the SR is stepwise decreased by interpolation in the spatial domain which results in a "contamination" of the mean colonocyte spectra by carbohydrates absorption bands (red arrows, see also Ref. [18] for details). The carbohydrates originate from mucin (muco- and glycoproteins) present as a precursor in goblet cells next to the colonocytes. Cluster mean spectra were obtained on the basis of agglomerative hierarchical clustering of a FT-IR imaging data set [18]. The uppermost spectrum (trace A) was derived from measured absorbance spectra with a spatial resolution of $8.8 \mu\text{m}$ at 4000 cm^{-1} .

The computational example of Figure 2 illustrates the need for standardizing the SR if spectral databases of reference spectra are collected. In order to achieve standardization of the SR we found it important to monitor the following measurement parameters and factors:

Geometry factors: in mapping experiments: step size in x- and y- direction, shape and diameter of the aperture; multichannel detectors: detector size and spacing of elements of a focal plane array detector.

Optical factors: shape and geometry of Cassegrain objectives, mirrors and field stops; transmission or transfection type measurements; confocal or non-confocal setup; chromatic aberrations introduced by the window material: thickness and refractive index of the supporting substrate; finally, the optical alignment of the IR microscope.

It is not the scope of this contribution to provide a comprehensive review of all factors with a potential impact on the SR in IR microspectrometry. For this the reader is referred to the literature [16,18].

5. Compilation of a spectral database for rapid screening and characterization of colorectal adenocarcinoma thin sections - An experimental example

5.1. The strategy of spectral analysis

In the following we will provide experimental data which exemplary demonstrate which strategies of spectral analysis are considered advantageous for the routine characterization of tissue sections by IR microspectrometry. The computational approach presented next should be rapid and practically useful in histology and histopathology, so that we defined the following criteria:

1. IR image segmentation should reflect the classical classification scheme in histology and histopathology. In the final stage of method development, precise definitions of parameters reflecting the degree of correspondence between the image segmentation method and histopathology (sensitivity, specificity etc.) should be available.
2. In order to be of practical use, IR imaging should be a rapid segmentation method that is applicable in routine use also for very large data sets. Ideally, the IR imaging method should run in time nearly linear in the number of image pixels. This is important as the CPU time of unsupervised agglomerative hierarchical cluster imaging which is frequently used in IR imaging scales with the squared number of pixels.

The general strategy of supervised classification analysis included the procedure of teaching and optimizing a multilayer perceptron artificial neural network (MLP-ANN) models followed by testing the classifiers with independent (external) validation data sets. Teaching and internal validation were carried out on the basis of IR microspectra from the colon database. External validation (testing) of the classifier was made by generating ANN images from complete infrared spectral maps. Thus, the classifiers were created with database spectra while model assessment was done by comparing the ANN images and the equivalent photomicrographs of post-stained tissue specimens (see Figure 3).

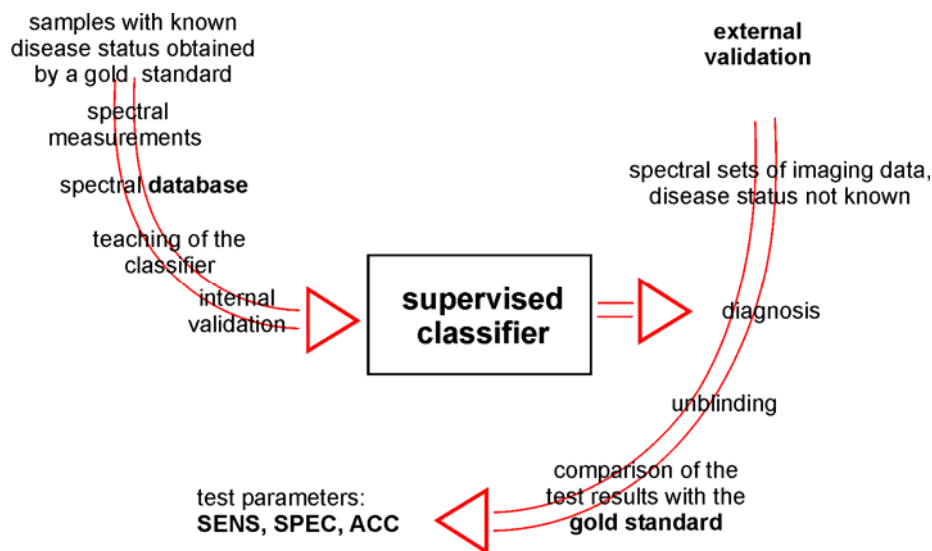


Figure 3. IR microspectroscopic imaging of tissues. The general strategy of supervised classification analysis.

5.2. Spectral preprocessing

Routine preprocessing of the raw spectral data aims to increase the robustness of classification by eliminating spectral outliers (quality tests) and compensate for quantitative aspects present in the spectra due to Beer-Lambert's law (normalization). We found furthermore, that methods of resolution enhancement such as derivation are effective and computationally less demanding procedures of spectral preprocessing which result in an increase of the accuracy of classification.

Quality test: Spectral quality tests of biomedical IR spectra were first introduced in the late 1980's within the context of a project for FT-IR analyses of intact microorganisms (see the contribution of D. Naumann "Twenty years of FT-IR on microorganisms at the RKI" in this volume). In these tests, the spectral "quality" is checked with regard to absorbance values of the raw spectral data, the signal to noise ratio (SNR) spectral contributions from water vapor, optical fringes and more. For IR microspectroscopic imaging we have adapted and expanded the quality test which consists now of five independent quality checks:

1. A test for spectral contributions of water vapor,
2. A check for sample thickness (integrated intensity),
3. The test of the spectral signal-to-noise-ratio (SNR),
4. A check called "test for an additional band" (tissue embedding medium)

5. A so called "bad pixel" test to eliminate spectra from dead pixels of focal plane array detector measurements.

Outliers, i.e. spectra that have failed one of the tests are routinely removed from the hyperspectral data sets and thus, are not accepted for multivariate classification analysis. The quality tests are an integral part of the CytoSpec software package that was designed for multivariate analysis of hyperspectral data sets. A detailed description of the quality checks is available at CytoSpec's website (see <http://www.cytospec.com/preproc.html#PreprocQuality>).

Spectral preprocessing: Spectra that have passed the quality tests can be subsequently processed for uni- or multivariate analysis. In classification analysis, the main goal of all preprocessing procedures is to remove the quantitative nature of the spectral information and to bring qualitative aspects of the IR spectra into the focus. It should be noted here that quantitative concepts of spectral analysis, for example to determine the concentration of a substance of interest in serum, will require completely different ways of spectral preprocessing. Thus, the conceptual design of the study defines the type of preprocessing that is applied.

An example of how spectral preprocessing affects the differentiability of spectra from different tissue structures in classification analysis is given in Figure 4. This illustration shows FT-IR point spectra from nine different structures of the human colon: spectra of the submucosa (green), crypts (red), and of seven other predefined tissue structures. The upper panel depicts the raw spectral data while spectra in the lower panel have been vector-normalized and offset corrected. In this simple case, characteristic spectral features of crypts (mucin features) and of the submucosa (features of collagen) are easily discernible from the preprocessed spectra, but not the raw data. Thus, the illustration demonstrates that spectral preprocessing, and normalization in particular, is indeed an essential prerequisite for classification analysis.

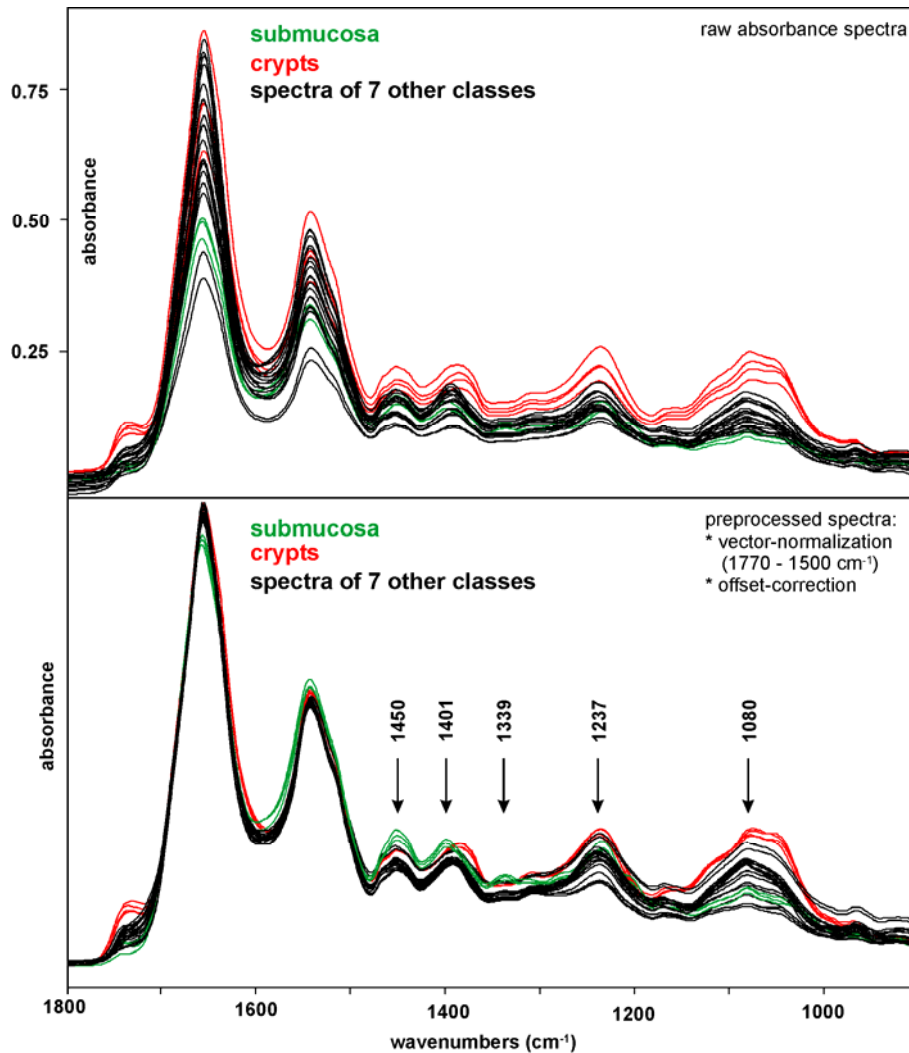


Figure 4. Example of spectral preprocessing for classification analysis of tissue spectra.

In more complex classification tasks we found the utilization of normalized first or second derivative spectra useful. The main advantage of derivative spectroscopy is the reduction of broad baseline effects and the enhancement of the spectral fine structure. Unfortunately, derivative spectroscopy requires a high SNR which is sometimes hard to achieve, particularly if the IR microspectra are acquired with high spatial resolution..

5.3. Unsupervised hierarchical cluster analysis of point spectra

Figure 5 displays the results of unsupervised agglomerative hierarchical clustering of a selection of individual tissue spectra from the colon database. The dendrogram illustrates that spectra from fat tissues can be easily differentiated from all remaining spectra which is certainly due to the presence of intense signals in the CH-stretching ($2800-3050\text{ cm}^{-1}$) and the carbonyl ester region ($\nu_{\text{sy}}>\text{C}=\text{O}_{\text{Ester}}$, 1737 cm^{-1}).

The dendrogram of Figure 5 shows furthermore, that also IR spectra of tissue structures containing mucin (crypts, spectra from extracellular "mucin lakes") and of the submucosa (cluster 4) form separate clusters. A closer inspection of IR spectra of cluster 1 yielded a number

of common spectral properties since these spectra displayed in the carbohydrate region typical spectral features of mucin (a mixture of muco- and glycoproteins). Furthermore, most of the differentiation of spectra from the submucosa is due to collagen which is known to exhibit a series of highly characteristic bands between 1100 and 1300 cm^{-1} [19]. To a lesser extent the latter statement holds true also for IR spectra of cluster 3, i.e. for spectra from distinct smooth muscle structures and fibrovascular connective tissue. These tissue types contain also collagen, so that the differentiation between clusters 3 + 4 and the remaining spectral classes (1, 2, 5) is perhaps due to bands of collagen. On the other hand, spectral signs from contractile elements of smooth muscle fibrils, which should be present only in the spectra of cluster 3, are apparently less discriminative.

We have noted that a number of spectra from the tunica muscularis and also from fibrovascular connective tissue appear in cluster 2. This may illustrate that clustering alone, i.e. without combination of any type of spectral feature selection, is not an optimal method to attain consistent classification results in IR microspectrometry of tissues. Although we will in the following demonstrate that supervised classification techniques have the potential to achieve a better correlation with histopathology, the approach of unsupervised HCA is considered as a valuable explorative tool in IR spectroscopy of tissues.

5.4. The use of supervised artificial neural networks (ANN) for image segmentation

In the following we wish to demonstrate how agglomerative hierarchical clustering (AHC) can be utilized in the design and developmental phases of a classification model. In particular we will show how the classification information provided by unsupervised HCA can be employed to establish a system of modular artificial neural networks suitable for classification of spatially resolved FT-IR microspectra. In the following example of Figure 6, a system of hierarchically organized artificial neural networks is given which consists of a so-called *top-level* ANN (see left part of Figure 6) and four specific *sub-level* ANNs (see right parts). While the *top-level* ANN assigns FT-IR spectra to one of the main colon tissue classes I-VI (see inset) the *sub-level* ANNs can subsequently perform more specific classification tasks (cf. Ia/b-IVa/b). ANN image segmentation follows the simple idea of assigning a distinct color to all spectra with an individual

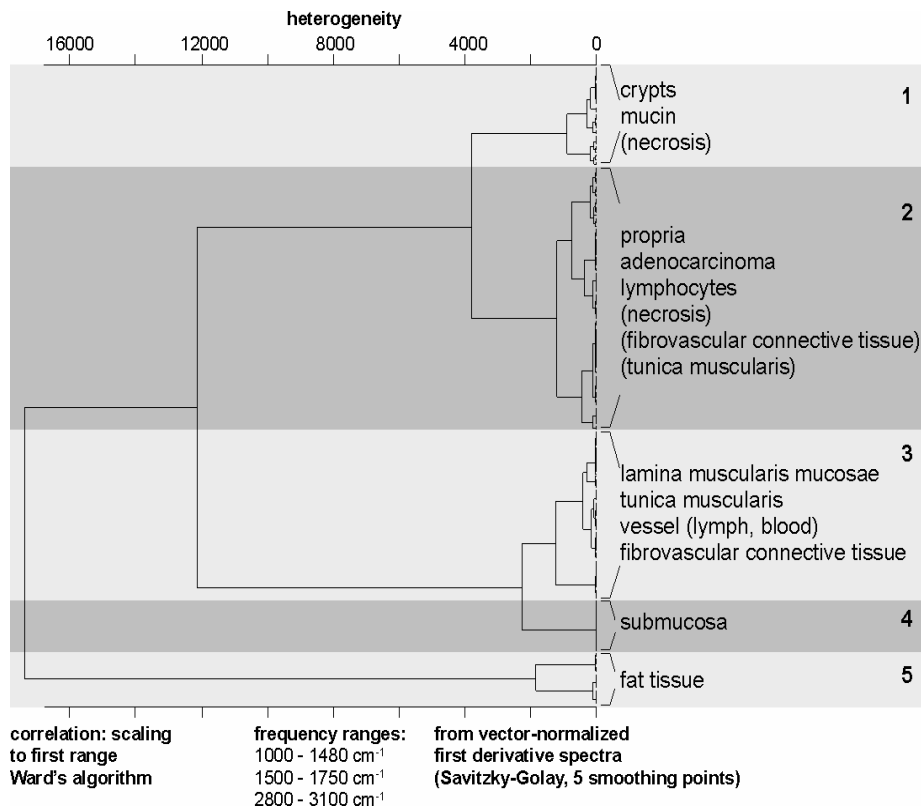


Figure 5. Dendrogram produced by unsupervised agglomerative hierarchical clustering (HCA) of representative FT-IR spectra from the colon database. The dendrogram illustrates that spectra from fat tissue and the submucosa can be easily differentiated from the majority of the database spectra. HCA classification of the remaining spectra yielded in a number of cases ambiguous results illustrating that unsupervised cluster analysis alone cannot be used to attain consistent classification results of databases (see text for details).

ANN class assignment. Since each spectrum of a mapping experiment has a unique spatial (x,y) position, false-color ANN images can be generated by plotting specifically colored pixels as a function of the spatial coordinates [8,9].

In the example of Figure 6 the classification information of AHC was used particularly for class definitions of the *top-level* net. For instance, cluster 5 (fat tissue) of the dendrogram of Figure 5 corresponds to class VI of the *top-level* ANN. Also, class I of the *top-level* ANN was defined on the basis of the class assignment of spectra from crypts and mucin by AHC. On the other hand, practical demands required in some instances to define additional *top-level* classes such as the class "adenocarcinoma". Class definitions for the *top-level* net were therefore made predominantly in view of spectral similarities of the tissues as revealed by unsupervised AHC, but considering also practical aspects of the method.

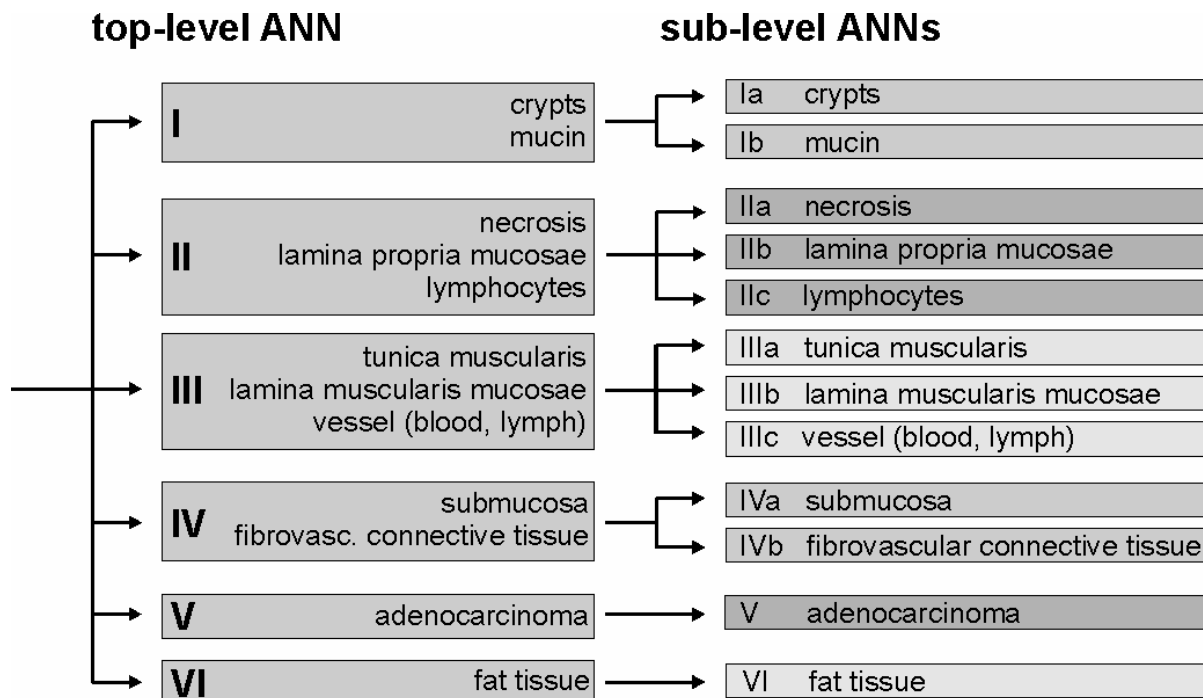


Figure 6. Example of a hierarchical (modular) classification scheme for ANN analysis of IR microspectra from the human colon. The combined classifier "combinet" consists of five individual ANN classifiers: a so-called *top-level* and four specific *sub-level* ANNs (see text for details).

The results of external (independent) validation of the ANN models is illustrated in Figure 7 showing ANN images produced by the top-level ANN and the "combinet" classifier, composed of one *top-* and four *sub-level* ANNs. While panel A of Figure 7 shows the photomicrograph of the unstained cryosection, panel B displays the same tissue area after staining with H&E. The widening of tissue clefts from A to B is due to water treatment during post-staining. In panels A-D the central shape is formed by necrotic tumor cells (1). These necrotic cells are surrounded by vital tumor epithelium (2). Neoplastic epithelium can be found also in the right parts of the images. All panels show furthermore non-cancerous fibrovascular connective tissue (3) which is arranged around the central adenocarcinoma structure, extracellular "mucin lakes" (4) and tissue clefts (5). As shown by Figure 7C and D, the main tissue structures of colorectal adenocarcinomas can be successfully identified by supervised ANN imaging. Note, that in this example the *top-* and *sub-level* ANNs have been trained with spectra of the database of pixel spectra (see Table 1). Microspectra of the actual tissue section B4205/94 were excluded from the teaching and internal validation data sets.

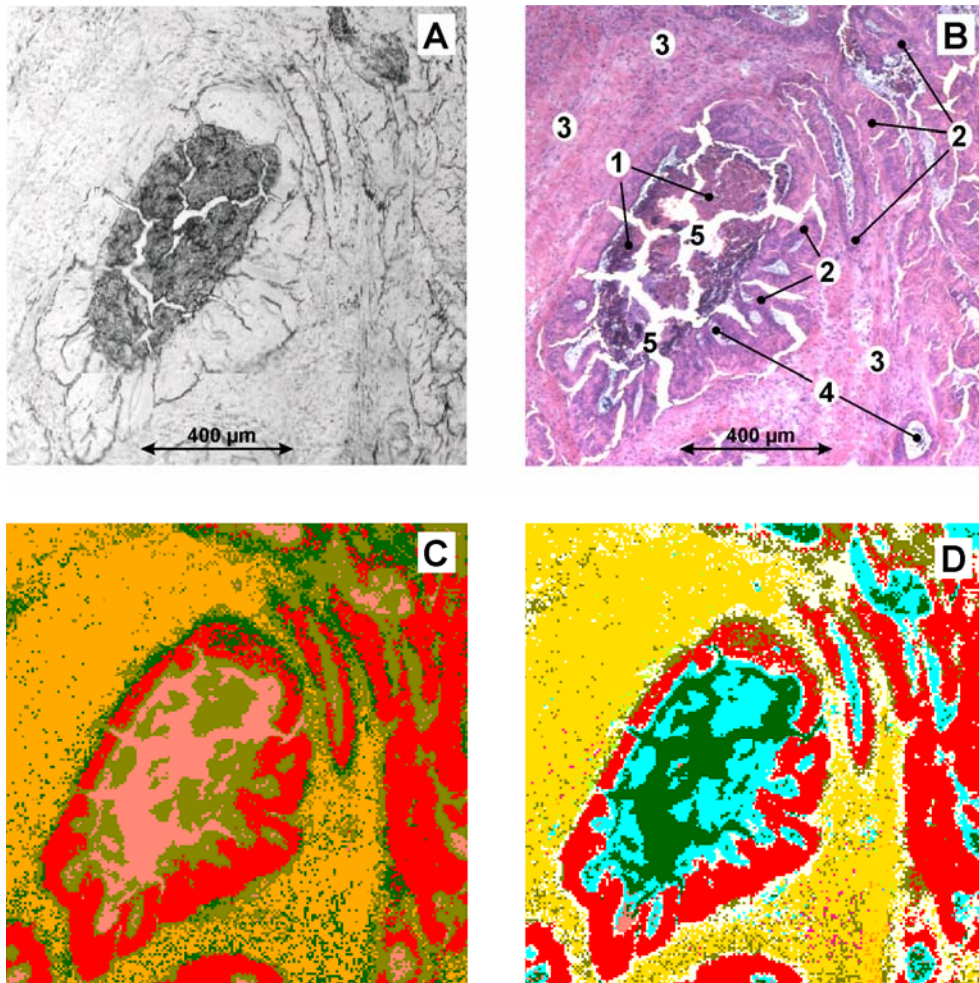


Figure 7. FT-IR microspectroscopic imaging of the cryostat section B4205/94 from a well differentiated (G1) adenocarcinoma of the rectum.

A Photomicrograph of the unstained cryostat section. Sample area: $1206 \times 1231 \mu\text{m}^2$ (194×198 spectra).

B Tissue area shown in A after IR microspectrometry and staining with H&E. 1 - necrotic detritus; 2- vital tumor cells; 3 - fibrovascular connective tissue and smooth muscle strands; 4 - secretion products (mucin); 5 - tissue clefts.

C IR imaging based on 192×194 microspectra of the tissue area shown in panels A and B and ANN analysis by the *top-level* ANN.

D Imaging based on FT-IR microspectrometry and ANN analysis ("combinet"). See text for details.

We now turn to a description of Figure 7C which was reassembled on the basis of the toplevel ANN classifier. In this image the class "mucin", probably secretion products in tissue clefts, is colored pink, whereas gold and red encode necrotic or vital tumor epithelium (classes II and V). Furthermore, a small number of pixel spectra was identified as smooth muscle structures (class III, dark green). Connective tissue structures from the submucosa or fibrovascular connective tissue (class IV) are colored orange. Although the class of connective tissue seems to be somewhat over-represented, the example of Figure 5C gives a good impression on the degree of correspondence between IR microspectrometry and histopathology and demonstrates the potential of ANN imaging for the analysis of tissue sections.

Panel D of Figure 7 shows the classification results obtained by ANNs with a hierarchically organized network architecture. In this example, the network "combinet" consisting of the *top-level* and four separate *sub-level* nets, was used to perform segmentation of the IR imaging data. The color class assignment as well as the number and percentage of spectra per class can be taken from Table 2. As it is shown in Figure 7D most of the predictions by the sub-level nets correlate quite well with histopathology. To give an example, spectra from the tissue clefts in the central shape of Figure 7D were classified by sub-level net #I as "mucin" (dark green). This seems to be correct, since we have stated earlier that these clefts contain mostly secretion products such as mucin, and cell debris. Furthermore, areas of necrotic tumor cells have been identified by sub-level net #II in accordance with histopathology as belonging to the class "necrosis" (aqua). On the other hand, sub-level net #II classified a large fraction of the spectra as "lamina propria mucosae" (light yellow). The classification of this particular class is probably incorrect. As it can be taken from Figure 7D, the class "lamina propria mucosae" is mostly found as a transitional state between the classes "adenocarcinoma" (red) and fibrovascular connective tissue, a class that is once again highly correlated with histology (gold).

	class name	color code	# of spectra	percentage [%]	mean activation
Ia	crypts	salmon	116	0.3	0.97
Ib	mucin	dark green	3313	8.62	1.00
IIa	necrosis	aqua	4567	11.89	0.98
IIb	lamina propria mucosae	light yellow	6189	16.11	0.98
IIc	lymphocytes	green yellow	201	0.52	0.90
IIIa	tunica muscularis	orange	73	0.19	0.91
IIIb	lamina muscularis mucosae	olive	3012	7.84	0.99
IIIc	vessel (blood, lymph)	deep pink	132	0.34	0.82
IVa	submucosa	blue	1	0	0.01
IVb	fibrovascular connective tissue	gold	11323	29.48	1.00
V	adenocarcinoma	red	9485	24.69	0.73
VI	fat tissue	beige	0	0	-
	unclassified spectra	black	0	0	-

Table 2. Classification results of the hierarchical ANN classifier "combinet" on FT-IR microspectroscopic imaging data obtained from a cryosection of a human colorectal adenocarcinoma (B4205/94). The corresponding IR image is given in Figure 7D. Color encoding in this figure was made according to the table content of columns 2 and 3.

Thus, the results of Figure 7D demonstrate in a exemplary manner the potentials, but also the problems the ANN imaging methodology is faced. It turned out that an adequate representation of all pre-defined spectral classes in the network's teaching phase is crucial for the optimization of the classification model of Figure 7. With reference to the example of Figure 7D, only sub-level net #II (and not the complete "combinet"-classifier) should be re-trained to improve the classifier.

Finally, it should be pointed out that also the type and the design of the classification model strongly influences the accuracy of prediction. The data suggest that a combination of small modular artificial neural networks gives the best performance. Modular classifiers are fast and the time which is required for classification scales linearly with the number of input patterns. Furthermore, modular ANNs can be trained and validated independently and are extendable at a

later stage for additional and more specialized classification tasks. Another advantage of modular ANN models is the fact, that individual *sub-level* ANNs can be specifically optimized to identify only a few (two) classes. This is particularly important since our model development strategy usually includes a procedure of detecting sets of discriminative spectral features. Thus, each of the individual ANNs can be optimized on the basis of pre-selected specific combinations of spectral features which will further increase the overall classification accuracy. Finally, each of the individual ANNs is principally adaptable in terms of sensitivity and specificity, i.e. the classifier can be specifically optimized to meet the particular needs of the application [see ref. 15 for details]. This high level of flexibility and the above mentioned advantages make the combination of feature selection and modular ANNs to ideal tools for routine use in IR microspectroscopic imaging of tissues.

6. Conclusions

The technique of mid-IR microspectroscopy and imaging has great potentials for rapid and reliable identification of tissue structures not only for scientific research purposes but also in a real clinical set-up. In this paper we discussed the question of standardization of the hyperspectral image acquisition protocol and we demonstrated how the interplay of unsupervised (HCA) and supervised classification techniques (ANN) can be utilized for classification model development. Preconditions for a successful application of the IR based tissue identification methodology are the standardization of measurement protocol (i), adequate data pre-treatment strategies (ii), feature selection (iii) and the development of supervised classification models (iv). Particularly, the concept of hierarchical, or modular network classification in combination with feature selection methods dramatically enhances the capabilities of IR based classification technique. We believe that the strategies outlined here may be successfully applied to a great variety of applications in biomedical spectroscopy, specifically in histopathology.

7. Acknowledgements

We are grateful to Max Diem, Melissa Romeo (Northeastern University Boston, USA), Dieter Naumann (Robert-Koch-Institut, Berlin, Germany) for fruitful discussions and support. Furthermore we would like to thank Jürgen Schmitt and Thomas Udelhoven from Synthon GmbH (Heidelberg, Germany) for the excellent collaboration.

8. Experimental Aspects

8.1. Sample preparation

Samples were stored until cryo-sectioning at a temperature of -80°C . Cryo-sectioning was performed at temperatures of -18 to -22°C . In order to avoid spectral contaminations associated with the use of embedding medium, the frozen tissue samples were mounted on the cryotome sample holder by means of freezing water. For FT-IR microspectrometry $8\ \mu\text{m}$ thin tissue slices were thaw-mounted onto CaF_2 windows of 1 mm thickness (Korth Kristalle, Germany). The specimens were stained after FT-IR measurements by Hematoxylin/Eosin and microphotographs of the imaged areas were obtained to correlate the IR images with histopathology. A detailed description of the histology and histopathology of colorectal adenocarcinomas can be found elsewhere [20].

8.2. Data collection

Infrared spectra were collected in transmission mode using a Spectrum Spotlight One FT-IR spectrometer from PerkinElmer coupled to a Spectrum Spotlight 300 infrared microscope. The microscope is equipped with a linear 16 x 1 element ($400 \times 15 \mu\text{m}^2$) MCT (HgCdTe) array detector. The microscope optics permits 1:1 or 4:1 imaging, resulting in sample areas of 25×25 or $6.25 \times 6.25 \mu\text{m}^2$ projected on each detector element. In this study spectra were recorded in the 4:1 imaging mode. In the 4:1 mode the lateral spatial resolution was found to be approximately $12 \mu\text{m}$ at $6 \mu\text{m}$ wavelength (corresponds to 1667 cm^{-1} , amide I region). A specially designed microscope box was purged by dry air to reduce spectral contributions from atmospheric water vapor and CO_2 . Nominal spectral resolution was 4 cm^{-1} . Usually, 16 scans were averaged per sample spectrum and apodized applying a Norton-Beer apodization function for Fourier transformation. Interferograms were zero-filled by a factor of 2. In order to increase the signal-to-noise-ratio background spectra were recorded with 512 scans.

8.3. Data processing

Spectral data were analyzed by means of CytoSpec (CytoSpec Inc. Croton-On-Hudson, NY, USA) and NeuroDeveloper (Synthon GmbH, Heidelberg, Germany). While CytoSpec is a software package specifically designed for the generation of infrared images from large IR mapping data, the NeuroDeveloper software combines modules for spectral feature selection, ANN model development (including modular ANN models) and ANN based classification. A detailed description of both software packages can be found elsewhere [21,22].

Spectral data were processed using a Fujitsu-Siemens 64 bit Celsius V810 workstation which is equipped with two 2.2 GHz AMD Opteron CPUs and 8 GB of RAM (Fujitsu-Siemens Computers GmbH, Germany). Microsoft Windows XP 64 bit version was chosen as the operating system since it provides significantly enlarged address space for application software.

Preprocessing of the raw spectral data included a conversion from transmittance to absorbance spectra, tests for spectral quality and normalization. The spectra quality test consisted of three separate checks: for water vapor content, for the signal-to-noise ratio (SNR) and for sample thickness. All spectra that have passed these tests were subsequently converted into first derivative spectra (Savitzky-Golay algorithm, 7 smoothing points) and vector normalized. Vector normalization was performed in the spectral region of $950\text{-}1480 \text{ cm}^{-1}$.

8.4. Unsupervised agglomerative hierarchical clustering

AHC was carried out on the basis of D-values (spectral distance measures) and Ward's algorithm (hierarchical clustering) [23,24].

8.5. ANN analysis

For network teaching, the data were preprocessed as already outlined and the effective spectral resolution was reduced by a factor of 6. Subsequently, 60-85 spectral features were chosen by a covariance analysis procedure implemented in the NeuroDeveloper software package [11]. We used connected three layer feed-forward MLP-ANNs consisting each of a layer of input, hidden, and output neurons. Teaching of the ANNs was carried out by utilizing the resilient backpropagation (rprop) algorithm [25]. The number of neurons of the input layer corresponds to the length of the input pattern and varied between 60-85. Moreover, the number of neurons in the hidden layer was usually set to four and the number of output neurons in MLP-ANNs equaled the number of classes.

ANN imaging on IR mapping data sets was carried out via a software interface between CytoSpec and the NeuroDeveloper software package. Based on NeuroDeveloper-ANN models, this interface can be used to perform image segmentation from the external validation data, i.e. complete infrared spectral maps. The interface is designed such that spectral preprocessing, feature selection and also ANN classification of the external validation data is automatically performed in the same way as for the teaching data.

(see <http://www.cytospec.com/image.html#ImageSYN> for details)

9. References

- [1] Harthcock M.A., Atkin S.C., Imaging with functional group maps using infrared microspectroscopy. *Appl Spectrosc.* 1988; **42(3)**: 449-455
- [2] Guilment J., Markel S., Windig W., Infrared Chemical Micro-Imaging Assisted by Interactive Self-Modeling Multivariate Analysis. *Appl. Spectrosc.* 1994; **48**:320-326.
- [3] Duponchel L., Elmi-Rayaleh W., Ruckebusch C., Huvenne J.P. Multivariate Curve Resolution Methods in Imaging Spectroscopy: Influence of Extraction Methods and Instrumental Perturbations *J. Chem. Inf. Comput. Sci.* 2003; **43**: 2057-2067
- [4] Choo L.P., Wetzel D.L., Halliday W.C., Jackson M., LeVine S.M. Mantsch H.H. In situ characterization of β -amyloid in Alzheimer's diseased tissue by synchrotron FTIR microspectroscopy. *Biophysical J.* 1996; **71**:1672-1679.
- [5] Kidder L.H., Kalasinsky V.F., Luke J.L., Levin I.W., and Lewis E.N. Visualization of Silicone Gel in Human Breast Tissue using new Infrared Imaging Spectroscopy. *Nature Medicine* 1997; **3**:235-237.
- [6] Kneipp J, Beekes M, Lasch P, Naumann D. Molecular changes of preclinical scrapie can be detected by infrared spectroscopy. *J Neurosci.* 2002; **22(8)**:2989-97.
- [7] Lasch P, Naumann D. FT-IR Microspectroscopic Imaging of Human Carcinoma Thin Sections Based on Pattern Recognition Techniques. *Cell Mol Biol.* 1998; **44(1)**:189-202.
- [8] Lasch P, Haensch W, Kidder L, Lewis EN, Naumann D. Colorectal Adenocarcinoma Characterization by Spatially Resolved FT-IR Microspectroscopy. *Appl Spectrosc.* 2002; **56 (1)**:1-9.
- [9] Lasch P, Wäsche W, Müller G, Naumann D. FT-IR Microspectroscopic Imaging of Human Carcinoma thin Sections. In: J.A. de Haseth (ed.): "Fourier Transform Spectroscopy: 11th International Conference" *AIP Conference Proceedings* 1998; **430**:308-311, Woodbury, New York
- [10] Lasch P, Haensch W, Naumann D, Diem M. Cluster Analysis of Colorectal Adenocarcinoma Imaging Data: A FT-IR Microspectroscopic Study. *Biochim Biophys Acta (BBA) - Molecular Basis of Disease*, 2004; **1688(2)**:176-186.
- [11] Udelhoven T, Naumann D, Schmitt J. Development of a Hierarchical Classification System with Artificial Neural Networks and FT-IR spectra for the Identification of Bacteria. *Appl. Spectrosc.* 2000; **54(10)**:1471-1479
- [12] Zell, A., Simulation Neuroner Netze. Addison-Welsey: Bonn, Paris, Reading, 1994
- [13] Marques de Sa J.P. Pattern Recognition: Concepts, Methods and Applications. Springer-Verlag: Berlin, Heidelberg, New York, 2001
- [14] Lasch P, Schmitt J, Beekes M, Udelhoven T, Eiden M, Fabian H; Petrich H, Naumann, D. Ante mortem Identification of BSE from Serum using Infrared Spectroscopy. *Anal Chem* 2003; **75(23)**:6673-6678
- [15] Lasch P, Diem M, Hänsch W, Naumann D, Artificial Neural Networks as Supervised Techniques for FT-IR Microspectroscopic Imaging. *J. Chemometrics* 2007, **20**. 209-220.
- [16] Carr, GL, Resolution limits for infrared microspectroscopy explored with synchrotron radiation. *Rev. Sci. Instrum.*, 2001, **72(3)**
- [17] Lasch P. Computergestützte Bildrekonstruktion auf Basis FT-IR mikrospektrometrischer Daten humaner Tumoren. Dissertation (ISBN 3-89820-030-2) 1999, Mensch & Buch Verlag, Berlin
- [18] Lasch P, Naumann D. Spatial Resolution in Infrared Microspectroscopic Imaging of Tissues, *Biochim Biophys Acta (BBA) - Biomembranes* 2006, **1758**. 814-829
- [19] Jackson M., Choo L-P., Watson P.H., Halliday W.C., Mantsch, H.H. Beware of Connective Tissue Proteins: Assignments and Implications of Collagen Absorptions in Infrared Spectra of Human Tissues. *Biochim. Biophys. Acta* 1995, **1270**:1-5.
- [20] Ponz de Leon M., Di Gregorio, C. Pathology of Colorectal Cancer, *Dig Liver Dis.* 2001; **33(4)**:372-88

- [21] NeuroDeveloper Website. <http://www.synthon-analytics.de> [01. May 2007].
- [22] CytoSpec Website. <http://www.cytospec.com> [01. May 2007].
- [23] Ward, J.H. Hierarchical Grouping to Optimise an Objective Function, *J. Americ. Stat Assoc.* 1963; **58**:236-244
- [24] Helm D., Labischinski H., Schallehn G., Naumann, D. Classification and Identification of Bacteria by Fourier-transform Infrared Spectroscopy. *J. Gen. Microbiol.* 1991; **137**: 69-79
- [25] Riedmiller M, Braun H. A Direct Adaptive Method for Faster Backpropagation Learning: The RPROP algorithm. In ICNN-93, *IEEE Intl. Conf. on Neural Networks*, San Francisco, CA, 1993; 586-591